Higgins, T. J. C., & Easterby, J. S. (1974) *Eur. J. Biochem. 45*, 147–160.
Inagami, T., & Sturtevant, J. M. (1960) *Biochim. Biophys. Acta 38*, 64–79.
Jones, J. G., Otieno, S., Barnard, E. A., & Bhargava, A. K. (1975) *Biochemistry 14*, 2396–2403.
Kosow, D. P., & Rose, I. A. (1971) *J. Biol. Chem. 246*, 2618–2625.
McDonald, R. C., Steitz, T. A., & Engelman, D. M. (1979) *Biochemistry 18*, 338–342.
Mesmer, R. E., & Baes, C. F., Jr. (1971) *Inorg. Chem. 10*, 2290–2296.
Ning, J., Purich, D. L., & Fromm, H. J. (1969) *J. Biol. Chem. 244*, 3840–3846.
Otieno, S., Bhargava, A. K., Barnard, E. A., & Ramel, A. H. (1975) *Biochemistry 14*, 2403–2410.
Pho, O. B., Rouston, C. R., Desvages, G., Pardel, L. A., & Thour, N. K. (1974) *FEBS Lett. 45*, 114–117.
Pickover, C. A., McKay, D. B., Engelman, D. M., & Steitz, T. A. (1979) *J. Biol. Chem. 254*, 11 323–11 329.
Purich, D. L., Fromm, H. J., & Rudolph, F. B. (1973) *Adv. Enzymol. Relat. Areas Mol. Biol. 39*, 249–326.
Redkar, V. C., & Kenkare, U. W. (1972) *J. Biol. Chem. 247*, 7576–7584.
Siano, D. B., Zyskind, J. W., & Fromm, H. J. (1975) *Arch. Biochem. Biophys. 170*, 587–600.
Subbarao, B., & Kenkare, U. W. (1977a) *Arch. Biochem. Biophys. 181*, 8–18.
Subbarao, B., & Kenkare, U. W. (1977b) *Arch. Biochem. Biophys. 181*, 19–25.
Viola, R. E., & Cleland, W. W. (1978) *Biochemistry 17*, 4111–4117.
Wilson, J. E. (1978) *Arch. Biochem. Biophys. 185*, 88–99.
Womack, F. C., & Colowick, S. P. (1979) *Proc. Natl. Acad. Sci. U.S.A. 76*, 5080–5084.

Resonance Energy Transfer between Catalytic Sites of Bovine Liver Uridine Diphosphoglucose Dehydrogenase†

James S. Franzen,* Paul S. Marchetti, and David S. Feingold‡

ABSTRACT: The catalytic-site thiol groups of three of the six identical subunits of bovine liver uridine diphosphoglucose dehydrogenase (EC 1.1.1.22) were alkylated with a fluorescent substituent that could serve as a donor in an energy-transfer donor–acceptor pair, and the catalytic-site thiol groups on the other three subunits were alkylated with a fluorescent substituent that could serve as an acceptor. The half-of-the-sites reactivity of the enzyme permitted introduction of the donor moiety at only three catalytic sites by reaction with 5-[[(iodoacetamido)ethyl]amino]naphthalene-1-sulfonic acid; doubly labeled enzyme was prepared by subsequent reaction with 5-(iodoacetamido)fluorescein, 5-(iodoacetamido)eosin, or 4-[*N*-(iodoacetoxy)ethyl-*N*-methylamino]-7-nitrobenz-2,1,3-oxadiazole. The specificity of labeling of the catalytic-site thiol groups was demonstrated by peptide mapping of tryptic digests of doubly derivatized enzyme. The magnitude of donor quenching was used to determine energy-transfer efficiencies. The equivalence of transfer efficiencies for the doubly labeled enzyme prepared by successive treatment with 5-[[(iodoacetamido)ethyl]amino]naphthalene-1-sulfonic acid and 5-(iodoacetamido)fluorescein measured by either donor quenching or sensitized fluorescence confirmed that energy transfer was responsible for the observed donor quenching. Theoretical models based on the known hexagonal-planar arrangement of the enzyme subunits and on the half-of-the-sites reactivity behavior of the enzyme are developed to permit calculation of the transfer efficiency as a function of the relative locations of the catalytic sites on the surfaces of the subunits. Comparison of the resulting maps of transfer efficiency vs. surface position with the observed transfer efficiencies allows designation of certain surface regions as likely locations of the catalytic sites. These results suggest that the catalytic sites of bovine liver uridine diphosphoglucose dehydrogenase are probably neither on those subunit surfaces that line the central cavity of the array nor in the intersubunit bonding domains. The preferred catalytic-site locations would be either the alternate poles of consecutive subunits or the outer peripheral regions of the hexagonal ensemble.

Bovine liver uridine diphosphoglucose dehydrogenase (UDPGDH;[1] EC 1.1.1.22) contains six identical 52 000-dalton subunits per native enzyme molecule (Gainey et al., 1972; Uram et al., 1972). As shown by electron microscopy, the six subunits of the hexamer are associated to form a hexagonal array (Franzen et al., 1980a). One of the 10–12 thiol groups per subunit is located in the catalytic site (Gainey et al., 1972; Uram, 1971) and is involved in covalent linkage with the partially and fully oxidized substrates during each enzyme turnover (Ridley & Kirkwood, 1973; Ridley et al., 1975). Furthermore, the enzyme shows half-of-the-sites behavior with respect to both substrate binding (Franzen et al., 1973; Gainey & Phelps, 1974) and reaction of the catalytic-site thiol group with modifying reagents (Franzen et al., 1976, 1978, 1980a).

The differential reactivities of the catalytic-site thiol groups provide a means for preparing altered enzyme molecules in which half of the catalytic sites are covalently bound to one particular substituent and the other half are bound to a dif-

† From the Department of Biological Sciences, Faculty of Arts and Sciences, University of Pittsburgh, Pittsburgh, Pennsylvania 15260. *Received May 12, 1980.* This work was performed in partial fulfillment of the Ph.D. degree requirements of P.S.M. at the University of Pittsburgh. It was supported by grants from the National Science Foundation (PCM 7708456) and the National Institutes of Health (AM 15332). This work was reported in part at the 2nd Biophysical Discussions meeting, Airlie, VA, May 1980 (Franzen et al., 1980c).

‡ Department of Microbiology, School of Medicine, University of Pittsburgh, Pittsburgh, PA 15261.

[1] Abbreviations used: UDPGDH, uridine diphosphoglucose dehydrogenase; BUP, *p*-(bromoacetamido)phenyl uridyl pyrophosphate; IAEDANS, 5-[[(iodoacetamido)ethyl]amino]naphthalene-1-sulfonic acid; IAE, 5-(iodoacetamido)eosin; IAF, 5-(iodoacetamido)fluorescein; IANBD, 4-[*N*-(iodoacetoxy)ethyl-*N*-methylamino]-7-nitrobenz-2,1,3-oxadiazole; TPCK, N^{α}-tosylmethylalanine chloromethyl ketone.

0006-2960/80/0419-6080$01.00/0

ferent substituent. If one of the substituents has spectral properties that would allow it to serve as the donor in a resonance energy transfer donor–acceptor pair and if the other substituent could serve as the acceptor, the derivatized enzyme might display resonance energy transfer, depending on the relative positions of the donor and acceptor moieties.

In this communication, we report experiments in which UDPGDH was labeled with fluorescent donor and acceptor reagents. To ensure that energy transfer was the mechanism responsible for any observed donor quenching, the transfer efficiencies of enzyme labeled with the donor–acceptor pair AEDANS–fluorescein were measured by two independent methods, donor quenching (Fairclough & Cantor, 1978) and sensitized fluorescence (Stryer, 1978). Transfer efficiencies were also measured by donor quenching with enzyme labeled with IAEDANS and IAE and with enzyme labeled with IAEDANS and IANBD. Application of certein structural inferences drawn from the half-of-the-sites-reactivity behavior of UDPGDH, the hexagonal-planar arrangement of the subunits, and a theoretical treatment that allows assignment of the probable location of the catalytic site to circumscribed subunit surface regions enabled us to extract topological information from the transfer efficiency numbers.

From these efforts, we conclude that the extended loci within which the catalytic sites of UDPGDH are situated are probably not on those subunit surfaces lining the central hole of the hexagonal-planar array nor in the intersubunit bonding domains but could be either on opposite poles of adjacent subunits or on the outer periphery of the ensemble.

Experimental Procedures

Materials. The enzyme was prepared and assayed as described by Zalitis & Feingold (1969) with modifications as indicated by Franzen et al. (1976). Purified enzyme had a specific activity of 3.5 units/mg where a unit refers to the μmol of UDPG oxidized per min; each batch was shown to be greater than 95% pure by densitometric scanning of Coomassie Blue stained sodium dodecyl sulfate–polyacrylamide slab gel electrophoretograms. Enzyme concentrations, reported as μN, were determined by using a molar subunit extinction coefficient of 51 000 L (mol-subunit)$^{-1}$ cm^{-1} at 277 nm.

[^{3}H]IAEDANS was synthesized as described by Huang et al. (1975) according to the method of Hudson & Weber (1973). The product gave a single fluorescent and radioactive spot when examined by thin-layer chromatography and ran identically with nonradioactive IAEDANS obtained commercially (Molecular Probes, Plano, TX). For use as a photochemically stable fluorescent standard, AEDANS was prepared by using the same method as above except that glacial acetic acid was substituted for iodoacetic acid. [^{14}C]IAF was prepared as described elsewhere (Franzen et al., 1980a).

Nonradiolabeled IAF, IAE, and IANBD were purchased from Molecular Probes, Plano, TX. BUP was received as a gift from Professor P. Frey of the Ohio State University (Wong et al., 1979).

Methods. Reaction of the native enzyme with radiolabeled thiol-specific reagents and measurement of the extent of covalent incorporation were carried out in the dark at pH 8.0 in 0.1 M potassium phosphate buffer 0.001 M in EDTA at 30 °C according to methods described previously (Franzen et al., 1976, 1980a). In these incorporation studies, the free-reagent concentrations were determined spectrophotometrically with the following extinction coefficients: IAEDANS and AEDANS, ϵ = 6100 cm^{-1} M^{-1} at 337 nm (Hudson & Weber, 1973); IAF, ϵ = 85 000 cm^{-1} M^{-1} at 491 nm (Mercola et al., 1972; Vanderkooi et al., 1977); IAE, ϵ = 92 500 cm^{-1} M^{-1} at 518 nm (gravimetrically determined); IANBD, ϵ = 32 500 cm^{-1} M^{-1} at 496 nm (gravimetrically determined); BUP, ϵ = 16 000 cm^{-1} M^{-1} at 258 nm (Wong et al., 1979). Incorporation of nonradiolabeled reagents was determined by spectrophotometric examination of samples of the reaction mixture which had been passed through a G-25 Sephadex column (5.5 × 0.6 cm) to remove free reagent. The absorbance at 277 nm was corrected for the dye absorption contribution by the relation $A_{277}^{prot} = A_{277}^{obsd} - fA_{dye}$, where A_{dye} was the sample absorbance at the wavelength of peak dye absorption. The factor f, which was determined from the absorption spectrum of the free dyes, has the following values: IAF, 0.24; IAE, 0.23; IANBD, 0.071.

Carboxymethylation of protein samples under reducing conditions, in preparation for peptide mapping studies, was carried out by standard procedures (Crestfield et al., 1963). The resulting carboxymethylated protein was digested with 1% of its weight of TPCK–trypsin (Worthington, Freehold, NJ) in 0.5% ammonium bicarbonate, pH 8.0, at 37 °C for 4–6 h. A second, equal addition of TPCK–trypsin was made, and the digestion continued overnight. The resulting clear digest was lyophilized and stored for subsequent peptide mapping.

The subsequent two-dimensional separations were carried out on paper (Bennett, 1967). The chromatograms were inspected with and without UV illumination, and the locations of any colored and/or fluorescent peptides were outlined. All of the peptides were then visualized by dipping papers into a cadmium–ninhydrin reagent (Dreyer & Bynum, 1967).

Fluorescence measurements were made at 25 °C with an Aminco–Bowman Model J4-8202G spectrophotofluorometer (American Instrument Co., Silver Springs, MD) equipped with a 4-8912 ratio photometer, but operated in manual mode using a spectral band-pass of 12 nm. The evaluations of the factors necessary to obtain corrected excitation and emission spectra were performed by standard methods (Chen, 1967; Argauer & White, 1964).

The quantum yield of fluorescence of IAEDANS–enzyme was determined by comparing the relative integrated corrected fluorescence intensities of the sample and quinine sulfate, 1 μg/mL, in 0.05 N H_2SO_4 (Parker & Rees, 1960). Integrated fluorescence intensities were computed by numerical integration at 10-nm intervals across the corrected emission spectra. A Wratten 1A filter in front of the entrance slit to the emission monochromator was used to eliminate second-order scattered light during recording of spectra. The quantum yield of quinine sulfate was taken to be 0.70 at 25 °C (Scott et al., 1970). The apparent quantum yield of IAEDANS–enzyme was multiplied by the factor $(4 - r)/4$, where r is the limiting anisotropy of IAEDANS–enzyme (see Table II; Shinitzky, 1972; Rao et al., 1979). Energy-transfer efficiencies were calculated according to the methodology described by Fairclough & Cantor (1978) and modifications thereof. In all cases, solutions with an optical absorbance of 0.03 or less were used so as to minimize inner filter effects and emission reabsorption by the samples. Although the donor fluorescence of enzyme labeled with both donor and acceptor was quenched relative to the fluorescence of donor enzyme alone, the band shape of the donor emission spectrum as well as the wavelength position of maximum intensity was unchanged, indicating that except for the quenching effect there was no significant perturbation of the donor due to the presence of the acceptor. Transfer efficiencies based upon this donor quenching effect were therefore calculated from the average ratio of the intensities of donor fluorescence across the donor emission bands of the two samples, or more simply from the ratio of the intensities at the emission wavelength maximum. Since the

donor was in all cases tritium labeled, the ratio of band intensities was corrected for differences in protein concentration between the two samples by normalizing the measured intensities of fluorescence by the number of counts in the respective samples. Hence, the transfer efficiency based on the donor quenching effect was calculated by eq 1

$$E = 1 - \frac{F_{DA}}{F_D}\frac{(cpm)_D}{(cpm)_{DA}} \quad (1)$$

where F_{DA} and F_D are the observed fluorescence intensities at the emission maximum of the donor in samples of donor–acceptor enzyme and donor enzyme, respectively, and $(cpm)_{DA}$ and $(cpm)_D$ represent the radioactivity of these two samples.

For the purpose of showing that the observed quenching of donor fluorescence by the acceptor was due primarily or exclusively to energy transfer according to the Förster mechanism, transfer efficiencies were also measured by sensitized fluorescence by recording the excitation spectrum of both donor enzyme and donor–acceptor enzyme. The excitation spectrum of acceptor fluorescence was monitored at a wavelength, λ_A, where the acceptor emission intensity was maximal. In this treatment, $G^{DA}_{\lambda_1}$ and $G^{DA}_{\lambda_2}$ were the magnitudes of the corrected emissions at λ_A of the donor–acceptor enzyme sample excited at two wavelengths, λ_1 and λ_2. The excitation wavelengths were chosen such that λ_2 was a wavelength where only the acceptor absorbed. Thus, for a sample containing both donors and acceptors, the following relationships held. At λ_1 where both donor and acceptor absorbed, but where the ratio of donor to acceptor extinction was maximal, the magnitude of the corrected excitation spectrum is given by eq 2. Similarly, for the same sample at λ_2 where only the acceptor absorbed, it follows that the magnitude of the corrected excitation spectrum is given by eq 3. E is defined as the transfer

$$G^{DA}_{\lambda_1} = A^{DA}_{A,\lambda_1}\phi_A + A^{DA}_{D,\lambda_1}E\phi_A + A^{DA}_{D,\lambda_1}(1 - E)\phi_D \quad (2)$$

$$G^{DA}_{\lambda_2} = A^{DA}_{A,\lambda_2}\phi_A \quad (3)$$

efficiency to be determined. A^{DA}_{A,λ_2} is the absorbance of the acceptor at λ_2 in the donor–acceptor complex and was determined directly from the absorption spectrum of the sample. A^{DA}_{D,λ_1} is the absorbance of the donor at λ_1 in the donor–acceptor enzyme and was calculated from the radioactivity in the sample and the extinction coefficient of the donor. However, A^{DA}_{A,λ_1}, the absorbance of the acceptor at λ_1 in the donor–acceptor sample, was not determined directly since the donor, turbidity, and the acceptor all contributed to the absorbance at this wavelength. A^{DA}_{A,λ_1} was therefore calculated as a fraction of the measured absorbance of the sample at λ_2, where the proportionality was computed from the absorption spectrum of the free acceptor dye in solution. Finally, the terms ϕ_A and ϕ_D are the apparent quantum yields, as observed at λ_A, for the acceptor and donor, respectively, in the donor–acceptor enzyme. ϕ_A is defined by the relation for $G^{DA}_{\lambda_2}$ just given, while ϕ_D is defined by $G^{D}_{\lambda_1} = A^{D}_{D,\lambda_1}\phi_D$ where $G^{D}_{\lambda_1}$ is the magnitude of the corrected excitation spectrum at λ_1 for donor enzyme alone, and A^{D}_{D,λ_1} is the absorbance at λ_1 of the donor in the donor enzyme sample, estimated from the radioactivity in the sample. From these relations, one can obtain the following expression (eq 4) for the transfer efficiency.

$$E = \frac{A^{D}_{D,\lambda_1}A^{DA}_{A,\lambda_2}G^{DA}_{\lambda_1} - A^{D}_{D,\lambda_1}A^{DA}_{A,\lambda_1}G^{DA}_{\lambda_2} - A^{DA}_{D,\lambda_1}A^{DA}_{A,\lambda_2}G^{D}_{\lambda_1}}{A^{D}_{D,\lambda_1}A^{DA}_{D,\lambda_1}G^{DA}_{\lambda_2} - A^{DA}_{D,\lambda_1}A^{DA}_{A,\lambda_2}G^{D}_{\lambda_1}} \quad (4)$$

If there happens to be no overlap of the donor emission band at the wavelength, λ_A, at which the acceptor fluorescence is being monitored, i.e., if $\phi_D = 0$, then $G^{D}_{\lambda_1} = 0$, and eq 4 reduces to eq 5, which has been given by Stryer (1978). Since with

$$E = \left[\frac{G^{DA}_{\lambda_1}}{G^{DA}_{\lambda_2}} - \frac{A^{DA}_{A,\lambda_1}}{A^{DA}_{A,\lambda_2}}\right]\frac{A^{DA}_{A,\lambda_2}}{A^{DA}_{D,\lambda_1}} \quad (5)$$

the donor–acceptor system employed in the present sensitized fluorescence energy transfer efficiency measurement there was a contribution of donor fluorescence at the wavelength, λ_A, at which the excitation spectrum of the acceptor was monitored, use of the slightly more complicated expression, eq 4, was necessitated. From the nature of this relation, it is evident that efficiencies determined by the sensitized fluorescence effect will be substantially less precise than those determined by donor quenching. The sensitized fluorescence method was only used therefore to establish that donor quenching was due to energy transfer.

The Förster critical distance, R_0, for each of the donor–acceptor pairs was calculated as usual by the standard relation (eq 6). The quantum yield for the donor, ϕ_D, in donor-labeled

$$R_0^6 = (8.79 \times 10^{-5})\kappa^2 n^{-4}\phi_D J \ (Å^6) \quad (6)$$

enzyme was measured as described earlier. The refractive index of the medium was taken as 1.4. The orientation factor, κ^2, was assigned to fall within a range of values, in accord with the considerations of Dale et al. (1979). However, many of the interpretive structural arguments are based on using the value of $^2/_3$ for κ^2. This matter is treated more fully under Discussion. The overlap integral, J, was computed from the following formula (eq 7)

$$J = \frac{\int_0^\infty F^{D}_{cor,\lambda}\epsilon_{A,\lambda}\lambda^4\, d\lambda}{\int_0^\infty F^{D}_{cor,\lambda}\, d\lambda} \ (cm^{-1}\ M^{-1}\ nm^4) \quad (7)$$

where $F^{D}_{cor,\lambda}$ is the magnitude of the corrected emission spectrum of the enzyme-bound donor in quanta per unit wavelength interval, $\epsilon_A(\lambda)$ is the molar extinction coefficient of the acceptor in M^{-1} cm^{-1}, and λ is the wavelength in nm.

Polarization measurements were carried out at 25 °C with a Glan–Prism polarizer assembly. The polarizations were calculated as given by Azumi & McGlynn (1962). Anisotropies were computed from the polarization values according to the relationship $r^{-1} = (p^{-1} - (1/3))(3/2)$. Limiting polarizations were determined from polarizations measured on solutions of the fluorophore-bearing molecule containing increasing concentrations of sucrose.

Results

As shown in Figure 1A (open circles), reaction of [^{3}H]-IAEDANS with native enzyme under pseudo-first-order conditions is distinctly biphasic, with the second slower, linear phase extrapolating to a zero-time value of 0.5 AEDANS group introduced per subunit. This demonstrates the half-of-the-sites reactivity character of this system, as has been discussed in greater detail in other reports (Franzen et al., 1976, 1978, 1980a), wherein it has been substantiated that the catalytic-site thiol is the site of initial reaction. This behavior is likewise shown in Figure 1A (open triangles) for IAF. In this particular experiment, the reaction was so rapid that the half-sites burst was over before the first sampling at 2 min. Other experiments, however, confirm the rapid half-sites reaction of IAF with UDPGDH (Franzen et al., 1980a). IAF and IANB show the same kinetic characteristics upon reaction with UDPGDH. In all these cases, loss of enzyme

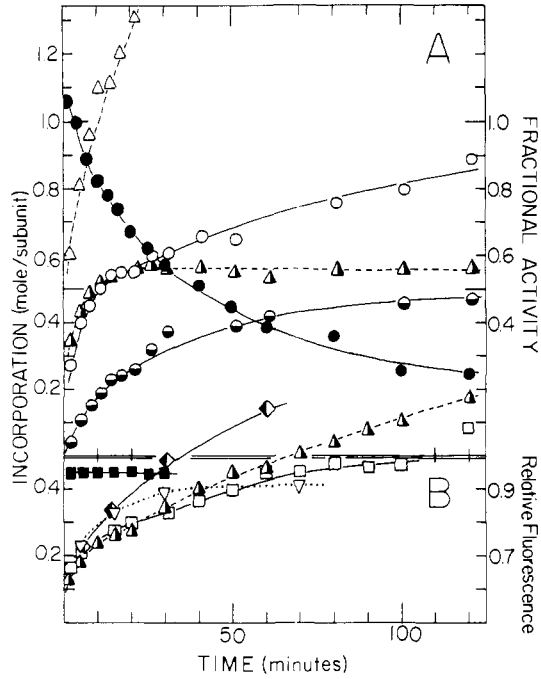

FIGURE 1: (A) Reaction of native UDPGDH with IAEDANS and IAF. All reactions were performed at 30 °C in 0.1 M potassium phosphate buffer, pH 8.0. Concentrations of enzyme and reagent are reported as μM enzyme subunits/μM reagent. Alkylations at high reagent concentrations: [^{3}H]IAEDANS, 6.8/340 (○); [^{14}C]IAF, 9.8/187 (△). Alkylations at low reagent concentrations: [^{3}HIAEDANS, 6.6/6.6 (◒); [^{14}C]IAF, 10.2/10.2 (▲). Loss of enzyme activity at low reagent concentration: [^{3}H]IAEDANS, 6.6/6.6 (●). (B) Reaction of half-sites IAEDANS with IAF, IAE, IANBD, and BUP: [^{14}C]IAF, 9.7/30 (▲); IAE, 23/22.5 (▽); IANBD, 23.4/58 (◆); [^{14}C]BUP, 9.3/137 (□). Fluorescence emission intensity (λ_{ex} = 340 nm, λ_{em} = 475 nm) of the sample reacted with BUP (■).

activity accompanies alkylation, and both alkylation and activity loss are repressed in the presence of substrate.

Figure 1A shows that at a 1:1 mole ratio of alkylating reagent to enzyme subunits the incorporation levels off at 0.5 per subunit (half-filled symbols). Since there is no significant loss of free reagent due to hydrolysis during the time required to reach the plateau incorporation levels, enzyme treated under these conditions is selectively modified at three of the six catalytic-site thiol groups. Enzyme reacted in such a manner with IAEDANS is referred to as "IAEDANS–enzyme." This procedure was used to prepare 25–50-mg batches of IAEDANS–enzyme, which was subsequently concentrated by ultrafiltration, dialyzed against storage buffer (0.2 M sodium acetate, pH 5.5, 2 mM in EDTA in 0.1 M mercaptoethanol), and stored at concentrations of 10–20 mg/mL until used. As shown in Figure 1A, such preparations of IAEDANS–enzyme had 20–25% of the catalytic activity of control enzyme (Franzen et al., 1980a). Although some precipitation of protein occurred with time, the properties of the enzyme remaining in the supernatant fraction remained constant for periods of several weeks. Molecular weight determinations by equilibrium centrifugation and electron micrographs of the derivatized enzyme confirm that the quaternary structure was basically unaltered by reaction with IAEDANS.

The fluorescence emission of AEDANS–enzyme (excitation at 340 nm) is maximal at 475 nm. In contrast, the free dye, AEDANS, has an emission maximum at 498 nm under the same solvent conditions. Urea denaturation of AEDANS–enzyme led to a 2-fold decrease of fluorescence and produced an emission spectrum virtually indistinguishable from that of the free dye in solution. Hence, covalent binding of the dye

Table I: Equilibrium and Kinetic Parameters for Ligand Interactions with Native UDPGDH and Half-Sites IAEDANS-UDPGDH

method and conditions	parameter	native enzyme	half-sites IAEDANS-enzyme
equilib dialysis: phosphate buffer, pH 8.0, 4 °C	no. of high-affinity UDPX binding sites	5.3	2.9
	K_{diss}^{UDPX} (μM)	3.8	5.3
steady-state kinetics: glycylglycine buffer, pH 8.5, 30 °C	K_m^{UDPG} (μM)	15.6	16.6
	$K_m^{NAD^+}$ (μM)	220	210
	K_I^{UDPX} (μM)	3.2	4.7
	k_{cat} (s^{-1})	2.6	0.5

to the native protein results in a shift in the position of maximum fluorescence to lower wavelengths and a substantial increase in quantum yield, consistent with findings of others (Hudson & Weber, 1973). Measurement, from corrected spectra, of the quantum yield of several IAEDANS–enzyme preparations (e.g., see Figure 5) gave a value of 0.97 after correction for the anisotropy effect. A quantum yield value of 0.97, though unaccustomably high, is not without precedent. For example, 9,10-diphenylanthracene in ethanol, *N*-methylacridinium chloride in water, and rubrene in *n*-heptane all have reported quantum yields of 1.0 (Parker, 1968).

Another factor, of somewhat uncertain magnitude, should be considered in the determination of the quantum yield of IAEDANS–enzyme. It has been shown that the extinction coefficient of IAEDANS is medium dependent [Table III of the paper by Hudson & Weber (1973)]. On the basis of the correlation between the extinction coefficient and the position of the maximum of the corrected emission spectrum, one can estimate that the extinction coefficient of the fluorophore in IAEDANS–UDPGDH may have increased from 6100 to 6850 M^{-1} cm^{-1} upon binding covalently. If such a change in the extinction coefficient had occurred, it would affect none of the calculated parameters used in this study, except the quantum yield of IAEDANS–enzyme. It is conceivable, therefore, that the proper quantum yield to be used in the determination of R_0 values is 0.86 [0.97 × (6100/6850)]. The net effect on the R_0 values of such an adjustment would be to reduce them by 2%.

The IAEDANS–enzyme has been further characterized with respect to its functional capacity. Equilibrium dialysis binding studies and limited steady-state kinetic analyses are summarized in Table I. Native and IAEDANS–enzyme showed competitive inhibition between UDP-xylose and UDP-glucose, but mixed inhibition of this inhibitor with NAD^+. From the entries of Table I, it can be affirmed that conversion of native enzyme to IAEDANS–enzyme removes three high-affinity UDP-xylose binding sites and, consistent with other studies (Franzen et al., 1980a), decreases the k_{cat} of the enzyme by 75–80%. These changes occur without significant effect on the apparent ligand binding affinities of the catalytic sites of unmodified adjacent subunits in the hexamer.

Further incorporation studies were undertaken in order to evaluate the specificity of labeling IAEDANS–enzyme with various other reagents. The incorporation profiles for the reaction of [^{14}C]IAF, -IAE, -IANBD, and -BUP with [^{3}H]-IAEDANS–enzyme are shown in Figure 1B. All these reagents eliminate the residual catalytic activity of IAEDANS–enzyme. However, with IAF and IANBD, the incorporations were not limited to 0.5 per subunit, and, hence,

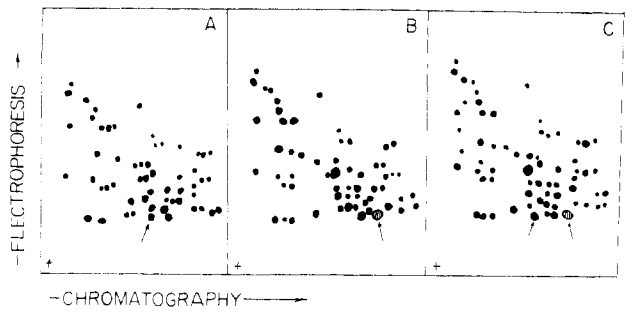

FIGURE 2: Peptide maps of fluorescent dye labeled UDPGDH. Samples of the enzyme were prepared as follows. Half-sites IAEDANS–enzyme (A) was prepared by reacting native enzyme in 0.1 M potassium phosphate buffer, pH 8.0, at 30 °C with [^{3}H]IAEDANS (1.2 mol of reagent/mol of subunit) until the activity was 25% of control. Typical reaction time was 60 min under these conditions. The reaction mixture was then subjected to gel filtration to separate modified enzyme from excess free dye. Half-sites IAF–enzyme (B) was prepared by similarly reacting native enzyme with IAF (0.8 mol of reagent/mol of subunit). The IAF incorporation determined spectrophotometrically was 0.56 per subunit. IAEDANS–IAF–enzyme (C) was prepared by labeling purified half-sites IAEDANS–enzyme at a total protein subunit concentration of 18.4 μM with 46 μM IAF for 60 min, at which time the preparation had negligible catalytic activity. The spectrophotometrically determined content of fluorescein was 0.56 per subunit. All samples were subsequently reduced, carboxymethylated, and digested with trypsin as described under Methods. After resolution of the peptides, 1.5 mg of samples, by descending chromatography and electrophoresis, the fluorescent peptides appearing on the dried maps were marked, and the sheets were developed with cadmium–ninhydrin reagent.

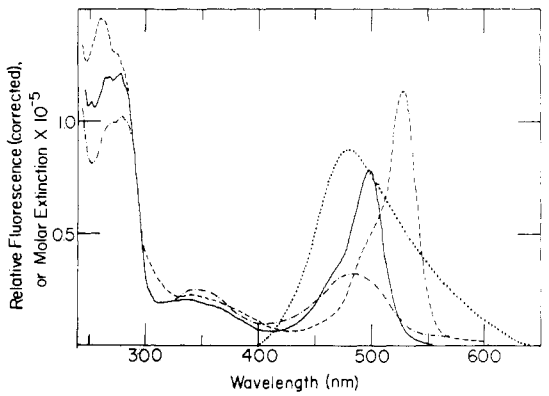

FIGURE 3: Absorption spectra of doubly labeled UDPGDH and corrected emission spectrum of half-sites AEDANS–UDPGDH. Spectra were all measured at 25 °C in 0.1 M potassium phosphate buffer at pH 8.0. Extinctions are presented on the basis of the molar concentration of dimers of enzyme subunits, moles of (enzyme subunit)$_2$(donor)$_1$(acceptor)$_{\sim 1}$ per liter. Absorption spectra: (UDPGDH)$_2$(–AEDANS) (–AF)$_{0.92}$ (—); (UDPGDH)$_2$(–AEDANS)(–AE)$_{1.23}$ (---); (UDPGDH)$_2$(–AEDANS)(–ANBD)$_{0.99}$ (----). Corrected emission spectrum: (UDPGDH)$_2$(–AEDANS)(–acceptor)$_{0.00}$ (···).

the extent of modification by the second reagent at sites other than the catalytic sites could not be discerned from the incorporation progress curves alone. Knowledge of the specificity of labeling with acceptor is gained from the results of peptide mapping of tryptic hydrolysates of modified enzyme, to be discussed. In general, when enzyme having three fluorescent donor groups and three fluorescent acceptor groups was prepared for energy-transfer studies, the concentration of the second reagent used was not in great excess, and the reaction was terminated when the incorporation of acceptor reached a value of 0.5 per subunit or slightly less.

Figure 1B also shows that IAEDANS–enzyme fluorescence was not quenched by modification of the remaining catalytic-site thiol groups with BUP, a compound which is nonabsorbing in the visible region of the spectrum. The null effect of BUP in IAEDANS–enzyme fluorescence indicates that the observed fluorescence quenching caused by the other reagents, IAF, IAE, or IANBD, was probably not simply the result of modification of the remaining catalytic-site thiols per se.

In Figure 2, the results of some of the various peptide mapping experiments are presented. These data permit evaluation of the specificity of labeling of the enzyme with the dyes employed for energy-transfer measurements. Panel A of Figure 2 shows the peptide map of enzyme modified to an extent of 0.5 with [^{3}H]IAEDANS. The arrow points to the single blueish fluorescent spot that appeared under ultraviolet radiation. A map of enzyme labeled to the extent of 1.2 per subunit with IAEDANS was essentially the same as map A, except for two additional minor fluorescent areas. The basic commonality of these two maps shows that the same site was alkylated in each reaction phase. The primary sequence of the alkylated tryptic peptide has been reported elsewhere (Franzen et al., 1980b). Also, these two map patterns indicate that incorporation of IAEDANS into native enzyme beyond the extent of three per hexamer could be carried out with a rather high degree of specificity for the catalytic-site thiol groups since there was a notable absence of any strongly fluorescent areas other than the one corresponding to the catalytic-site peptide.

Panel B of Figure 2 represents the tryptic peptide map of enzyme labeled at three of the six catalytic sites with IAF. Map B demonstrates that the catalytic-site peptide bearing fluorescein (arrow), yellow under natural light and bright green-yellow under ultraviolet light, has a greater chromatographic mobility than when derivatized with IAEDANS. Panel C displays the tryptic peptide map of half-sites IAEDANS–enzyme labeled with IAF to an extent of three bound fluorescein groups per hexamer. Interestingly, this map showed two discrete highly fluorescent spots (arrows). The less mobile spot had a blueish fluorescence and corresponded to the IAEDANS–peptide of panel A. The faster moving fluorescent spot was yellow colored and fluoresced green-yellow. Comparison of maps B and C shows that the IAF–peptides migrate to the same position whether they derive from the first stage of protein modification (map B) or the second stage (map C). This was demonstrated more convincingly by doing a two-dimensional separation (not shown) of a 1:1 mixture of the enzyme digests used to prepare maps B and C. A single IAEDANS–peptide and a single IAF–peptide were seen in the map of the mixture. From these mapping data, we conclude that the same thiol group was modified in both stages of the alkylation reactions and that under the conditions used to label the second class of sites the incorporation is predominantly selective for the remaining three catalytic sites.

The absorption spectra of the donor–acceptor-labeled enzymes, normalized to equivalent concentrations of enzyme, are shown in Figure 3. Also drawn in Figure 3 is the corrected emission spectrum of IAEDANS–enzyme, qualitatively illustrating the magnitude of overlap of this emission with the three acceptors used.

Figure 4 provides an example of the quenching effect produced by introduction of fluorescein acceptor groups at the remaining three catalytic sites of IAEDANS–enzyme. It is apparent from the two spectra of the doubly labeled protein has only half as much fluorescence at 475 nm as the IAEDANS–enzyme. The emission spectrum of IAF–enzyme (excitation at 340 nm; see Figure 4) demonstrates that acceptor emission intensity was negligible below 485 nm. Therefore, effects on the fluorescence observed at 475 nm were uncom-

Table II: Summary of Parameters Relating to Energy-Transfer Studies

method	parameter	sample: IAEDANS-enzyme	IAEDANS-IAF-enzyme	IAEDANS-IAE-enzyme	IAEDANS-IANBD-enzyme
limiting polarization (P_0)	donor	0.170	0.170	0.175	0.158
	λ_{ex}-λ_{em}	340–475	340–475	340–475	340–475
	acceptor		0.211	0.281	0.321
	λ_{ex}-λ_{em}		460–525	500–540	490–525
limiting anisotropy (r_0) (protein)	donor	0.120	0.120	0.124	0.111
	acceptor		0.151	0.207	0.241
fundamental anisotropy (r_f) (free dye)	donor	0.214[a]	0.214	0.214	0.214
	acceptor		0.40[b]	0.40[c]	0.40[d]
depolarization factors	$\langle d_D \rangle$	0.561	0.561	0.579	0.519
	$\langle d_A \rangle$		0.378	0.518	0.603
	$\langle d_D^x \rangle$	0.749	0.749	0.761	0.720
	$\langle d_A^x \rangle$		0.614	0.719	0.776
orientation factors	κ^2_{min}		0.21	0.17	0.16
	κ^2_{max}		2.5	2.7	2.8
overlap integral (M^{-1} cm^{-1} nm^4)	$J_{DA} \times 10^{-15}$		1.82	2.03	1.14
Forster critical distance (Å)	$R_0^{(2/3)}$		55.1	56.1	50.9
	R_0^{min}		45.4	44.6	40.1
	R_0^{max}		68.6	70.8	64.7
transfer efficiency[e]	$\bar{E}^0$		0.46 ± 0.05	0.32 ± 0.03	0.32 ± 0.03

[a] Hudson & Weber, 1973. [b] Chen & Bowman, 1965. [c] Cherry & Schneider, 1976. [d] In the absence of literature data for the fundamental anisotropy for IANBD, a value of 0.40 is assumed. [e] From Figure 6 for an incorporation of 0.5 acceptors/subunit.

plicated by fluorescence contributions from the acceptor. Although the corresponding spectra are not shown, the observations just described for IAEDANS–IAF–enzyme were, in principle, the same for IAE and IANBD as acceptors.

The transfer efficiencies, evaluated from the magnitude of donor quenching such as shown in Figure 4, were determined on samples of IAEDANS–enzyme having different levels of incorporation of any one of the three acceptors IAF, IAE, or IANBD. Typical results of transfer-efficiency measurements made at various stages of acceptor incorporation into IAEDANS–enzyme are displayed in Figure 5. The transfer efficiencies corresponding to an acceptor incorporation of 0.5 per subunit have been obtained from these plots for each of the three donor–acceptor pairs and therefore represent the average transfer efficiency due to all interactions of three donors and three acceptors on the enzyme hexamer.

In order to demonstrate that the IAEDANS–enzyme fluorescence quenching effect shown in Figure 4 was due to energy transfer from IAEDANS to IAF, transfer efficiencies based on sensitized fluorescence measurements were made as described under Methods. The results of these measurements of five separate samples appear in Figure 5 as the five sets of paired half-filled circles: upper half filled, donor quenching; lower half filled, sensitized fluorescence. Comparable efficiencies are obtained, it appears, regardless of the method from which they were derived, thus confirming that the donor quenching effect of covalently bound fluorescein (and presumably the other acceptors, eosin and the NBD moiety) on IAEDANS–enzyme was due primarily, if not exclusively, to resonance energy transfer according to the Förster mechanism.

Measurements of the fluorescence polarization of the IAEDANS–enzyme over a wide range of sucrose concentrations showed that this parameter was unaffected by solvent viscosity, indicating that the rotational correlation time of the IAEDANS–enzyme hexamer was large relative to the lifetime of the excited-state dye. Hence, the macromolecule is effectively immobilized on the time scale of the experiment. The polarizations of the acceptors in donor–acceptor-labeled enzyme were also measured. Since the rotational correlation time

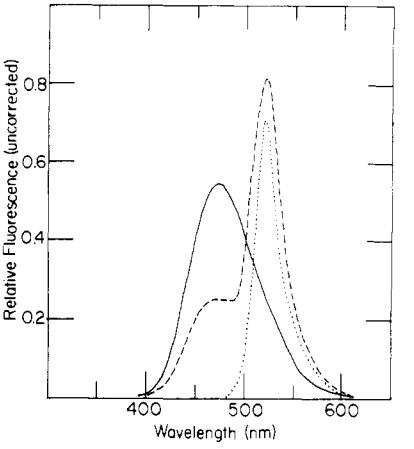

FIGURE 4: Fluorescence properties of half-sites IAEDANS–UDPGDH, IAEDANS–IAF–UDPGDH, and half-sites IAF–UDPGDH. Fluorescence emission spectrum (λ_{ex} = 340 nm) of half-sites IAEDANS–enzyme at a subunit concentration of 1.3 μM (—). Spectrum of IAEDANS–IAF–enzyme at the same subunit concentration (- - -). The IAF incorporation was 0.53 per subunit for this sample. Fluorescence emission spectrum (λ_{ex} = 340 nm) of half-sites IAF–enzyme at a subunit concentration of 0.93 μM (···).

of the enzyme was demonstrably large, the observed polarizations of the enzyme-bound acceptors were considered equal to the polarizations of these moieties uninfluenced by rotation of the protein as a whole (i.e., the limiting polarizations of Table II).

Table II summarizes the appropriate Förster critical distances, the parameters needed to evaluate these critical distances, and the values of the observed transfer efficiencies for the three fully donor–acceptor-labeled enzymes. The recommendations of others regarding the treatment of the elusive orientation factors have been followed by evaluating κ^2_{min} and κ^2_{max}, see Table II (Dale et al., 1979).

Discussion

From the observed transfer efficiencies and corresponding R_0 values of Table II, one can qualitatively conclude that the

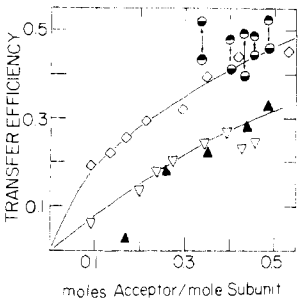

FIGURE 5: Energy-transfer efficiencies for IAEDANS–acceptor–UDPGDH as a function of acceptor incorporation. Samples of [^{3}H]IAEDANS–enzyme at subunit concentrations of about 20 μM were reacted with moderate excesses of IAF (◇), IAE (▽), or IANBD (▲) over a total time period of 60–90 min. Aliquots were removed from the reaction mixture at various times and applied to G-25 Sephadex columns for resolution of free dye from enzyme. Acceptor incorporations were determined for the purified enzyme by spectrophotometric measurement of acceptor optical absorbance and radioactivity measurement of [^{3}H]IAEDANS–enzyme. Transfer efficiencies were determined for these samples from the fluorescence intensity at 475 nm, excited at 340 nm, based on the donor quenching method as described under Methods. The circles represent paired transfer efficiency measurements of five separate preparations made by the donor quenching method (◓) and the sensitized fluorescence method (◒).

catalytic sites of UDPGDH are probably well separated. It is unlikely that the sites of two adjacent subunits are in or near their common bonding domain. However, since the system under study is complicated by the simultaneous presence of three donor groups and three acceptor groups per hexamer, it is appropriate to develop a system of analysis, albeit crude, for making structural statements from the energy-transfer measurements.

There seem to be two reasonable models which to a first approximation are consistent with the demonstrated properties of UDPGDH. As stated in the introduction, the enzyme is hexameric, displays a hexagonal-planar appearance on electron micrographs, and manifests half-of-the-sites behavior with respect to noncovalent ligand binding and covalent modification. These facts, and the generally accepted principle that protein subunits associate so as to form oligomers which can be assigned to point-group symmetry classes (Klotz et al., 1975; Matthews & Bernhard, 1973), allow us to propose that (1) the UDPGDH molecule is a trimer of dimers (half-of-the-sites reactivity is an intradimer effect) and (2) the UDPGDH molecule can be assigned either of two point-group symmetries: point-group symmetry 32 (or D_3) (model A; all six intersubunit bonding domains are homologous); point-group symmetry 3 (or C-3) (model B; all six intersubunit bonding domains are heterologous). If each subunit can be essentially contained in a spherical envelope, the models might be envisioned by the following representations:

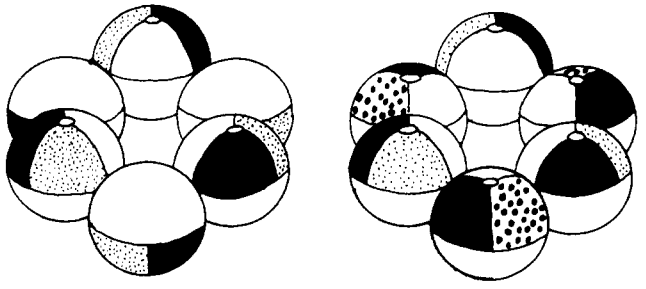

model A model B

Note that model B, in which all the subunits have the same primary structure but alternate ones have different conformations, is an example of what is sometimes known as a preexisting asymmetry system. The positions of the six catalytic sites in space would still conform to point-group 6, but the distortions in alternate subunits, which are the source of the different catalytic-site thiol reactivities, lower the high-resolution symmetry to 3. It is unlikely that the hexagonal array of subunits has true 6 (or C-6) symmetry since there would then be no easy way to account for the half-of-the-sites reactivity displayed by UDPGDH toward so many reagents (Franzen et al., 1980a). We have no a priori reason to prefer model A over model B nor, as will be seen, do the results of this study lead to developing any such preference.

The hexagonal ensemble of subunits may be likened to a hexagonal array of geographical globes, each having its equator in the plane of centers of the array and its prime meridian directed toward the center of the array. For model A, 32 symmetry, the north poles of every other subunit would point up. For model B, 3 (or pseudo-6) symmetry, all the north poles would point up. The location of any surface point on one globe by angles of latitude, ϕ, or longitude, θ, fixes the like points on the other globes and determines all of the intersite distances. For the sake of reference, if positive ϕ is considered to be north, positive θ would correspond to positions east of the prime meridian. Moreover, for the 32-symmetry arrangement (model A), the intradimer bonding domain (through which half-sites reactivity effects would be transmitted) corresponds to the contact between western hemispheres at $\phi = 0°$, $\theta = -60°$. For model B, the contacts all involve the $\phi = 0°$, $\theta = +60°$ point on each sphere with the $\phi = 0°$, $\theta = -60°$ point on the next sphere.

To account for half-of-the-sites reactivity, it is reasoned for model A that labeling of the native enzyme with donors occurred randomly with respect to which dimer in the trimer of dimers was modified, but that once one of the subunits of a dimer was modified that other site was refractory. Sbusequent labeling with acceptor to produce the fully modified enzyme, ED_3A_3, would then yield a 1:3 mix of the two forms, form I and form II, shown schematically below. In form I, all three

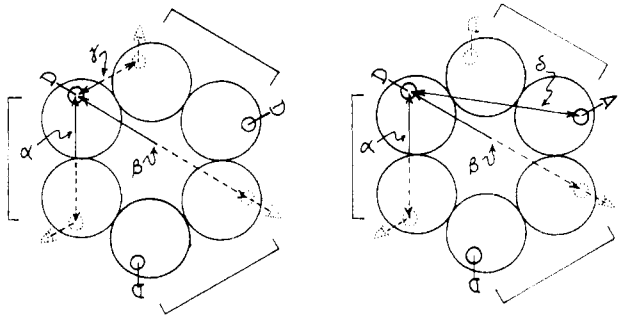

I II

donors are on the same side of the plane of the 2-fold axes. In form II, only two donors are on the same side of this plane. Since there are three ways of achieving the latter arrangement, 3!/(2!)(1!), and only one for the former, 3!/(3!)(0!), form II would predominate 3:1.

The above forms also serve to identify the four possible normalized donor–acceptor distances for model A. These distances are related to the angles ϕ and θ by eq 8.[2]

$$\alpha_{32} = 2\{[1 - \cos\phi\cos(\theta + 60°)]^2 + \sin^2\phi\}^{1/2}$$

$$\beta_{32} = 2\{[2 - \cos\phi\cos\theta]^2 + \sin^2\phi\}^{1/2}$$

$$\gamma_{32} = 2\{[1 - \cos\phi\cos(\theta - 60°)]^2 + \sin^2\phi\}^{1/2}$$

$$\delta_{32} = \{3[4(1 - \cos\phi\cos\theta) + \cos^2\phi]\}^{1/2} \qquad (8)$$

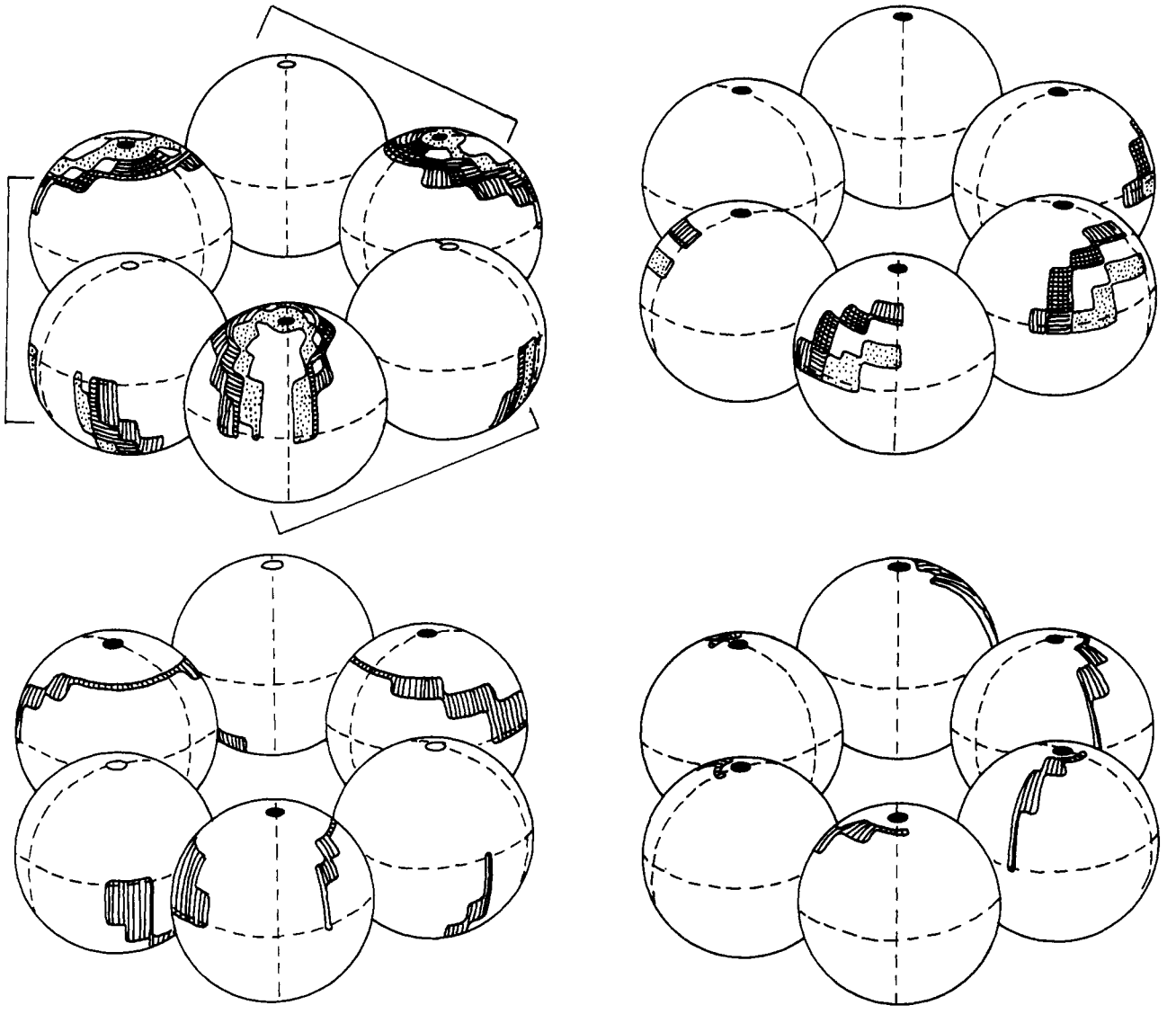

FIGURE 6: Displays of loci of catalytic-site regions of UDPGDH determined by energy-transfer measurements. Upper: Allowed regions within which the catalytic sites of UDPGDH might be located as determined by using R_0 ($^2/_3$) values for the Förster critical distances, as described under Discsussion. The differently marked areas correspond to the three different donor–acceptor-labeled samples used: vertically lined, IAEDANS–IAF; horizontally lined, IAEDANS–IANBD; stippled, IAE; crossed, overlap of IAEDANS–IAF and IAEDANS–IANBD areas. The left-hand figures correspond to the 32-symmetry model (model A) where the subunits in the pairs marked as dimers are connected through the domain that presumably transmits the half-sites reactivity effect. The right-hand figures correspond to the 3-symmetry (pseudo-6-symmetry) model (model B). For either of these cases, the mirror images of the figures shown would also be acceptable representations. The handedness of these depictions rests on the arbitrary initial definition of the coordinates. Lower: Allowed catalytic-site regions for the models A (left) and B (right) by using R_0(min) values for IAEDANS–IAF.

Similarly, for model B, one obtains relations between the normalized intersite donor–acceptor distances and the angles ϕ and θ. Since the two kinds of subunits are accorded different reactivities toward the donor reagent IAEDANS (half-of-the-sites reactivity), one obtains a sample in which essentially all of the molecules bear donors and acceptors on alternate subunits, respectively. The appropriate equations therefore are those of eq 9 (note that the distance δ_3 does not exist as a donor–acceptor distance in model B).

Energy transfer along any one of the distances, α, β, etc., should probably be characterized by its own orientation factor value, $\kappa^2_{\alpha_{32}}$, for example. Such detailed knowledge is not available, however; and therefore a single estimate of κ^2 and R_0 has been employed for each type of donor–acceptor pair studied. Since there is some motional freedom fo the fluorophores and since the AEDANS emission is mixed (Hudson & Weber, 1973), a common value of κ^2 for all the intersite donor–acceptor distances is a reasonable approximation. We next define a parameter ρ as the ratio of R_0 to the radius of a spherical subunit, the latter being calculated from the partial specific volume and molecular weight of the subunit. For these studies, the subunit radious was taken to be 25 Å. For fully donor–acceptor-labeled enzyme, the transfer efficiencies can then be calculated in terms of the site location, defined by θ and ϕ, according to eq 10 and 11 for models A and B, respectively.

$$\alpha_3 = \gamma_3 = \{4[1 - \cos\phi\cos\theta] + \cos^2\phi\}^{1/2}$$
$$\beta_3 = 2\{[2 - \cos\phi\cos\theta]^2 + \cos^2\phi\sin^2\theta\}^{1/2}$$
$$\delta_3 = \delta_{32} \qquad (9)$$

[2] The derivation of general distance relations (e.g., eq 8 and 9 are special cases) for oligomers having any number of subunits in either dihedral or cyclic symmetry arrangements has been developed by J.S.F. and Professor Robert B. Griffiths, Physics Department, Carnegie-Mellon University. The results are obtainable upon request from the corresponding author.

$$E_A = 0.25\{[1 + \rho^{-6}(\alpha_{32}^{-6} + \beta_{32}^{-6} + \gamma_{32}^{-6})^{-1}]^{-1} + [1 + \rho^{-6}(\alpha_{32}^{-6} + \beta_{32}^{-6} + \delta_{32}^{-6})^{-1}]^{-1} + [1 + \rho^{-6}(\alpha_{32}^{-6} + \gamma_{32}^{-6} + \delta_{32}^{-6})^{-1}]^{-1} + [1 + \rho^{-6}(\alpha_{32}^{-6} + 2\delta_{32}^{-6})^{-1}]^{-1}\} \quad (10)$$

$$E_B = [1 + \rho^{-6}(\alpha_3^{-6} + \beta_3^{-6} + \gamma_3^{-6})^{-1}]^{-1} \quad (11)$$

With these equations, efficiencies were calculated for the fully labeled enzyme at 15° intervals of ϕ and θ. To illustrate the application of the results of these calculations, Figure 6 was constructed, in which are drawn the hexagonal ensembles of spheres arranged according to either model A (upper left) or model B (upper right). The marked areas correspond to regions where the efficiencies calculated according to the equations just given for E_A and E_B fall within 10% (estimated reliability of measured efficiencies) of the observed efficiencies for the samples of IAEDANS–enzyme labeled fully with either IAF, IAE, or IANBD. The significant conclusion apparent from Figure 6 is that, regardless of the symmetry of the model used to describe UDPGDH, the surface regions allowed by the energy-transfer efficiency values for locating the catalytic site are neither in the central region of the hexamer nor in the intersubunit bonding domains. The catalytic sites are more likely to be found on the periphery of the aggregate or on alternate poles of adjacent subunits.

The conclusion that the central hole and the intersubunit domains are to be excluded from consideration as catalytic-site loci is not seriously dependent on the values of R_0 employed. For example, in the lower row of Figure 6, one sees the effect of using R_0(min) values (see Table II) for the calculations. Although the allowed regions move toward the central hole and the intersubunit domains, they do not extend to these regions. The correct values of R_0 are probably larger than the R_0(min) values used to generate the lower part of Figure 6. The calculation of the R_0(min) values was based on the premise that both the donor and acceptor transitions are pure (Dale et al., 1979). However, because the polarization across the IAEDANS emission band is variable, this transition is most likely mixed (Hudson & Weber, 1973). Hence, the appropriate orientation factors for the three acceptors paired with this donor in the current study are not likely to be as small as those giving rise to the R_0(min) values of Table II (Haas et al., 1978a,b). In turn, our general conclusions about regions in which it is unlikely to find the catalytic sites are reinforced. The use of R_0(max) values (Table II) results in the calculated efficiencies over all map regions, substantially higher than the measured efficiencies. Hence, the correct value of R_0 must be smaller than R_0(mas). The net result of these considerations is that a reasonably useful picture of the catalytic-site loci is probably obtained by using the values of $R_0(^2/_3)$ as the Förster characteristic distances for the donor–acceptor pairs.

Although the results of the calculation are not shown, the general conclusion about the restricted locations of the catalytic sites already drawn is not affected by relaxing the constraint of model A that no interdimer interaction influences the labeling with donor. Recall that labeling of enzyme with IAEDANS was assumed to proceed randomly on the three dimers, but only one site per dimer was considered to have been blocked. The consequence of this constraint was that 75% of the sample was of the form II type and 25% of the form I type. It the sample is considered to be either all form I or all form II, the allowed regions shift in position; however, they still invade neither the interior hole nor the intersubunit domains.

The interpretive models developed herein have so far been used for the calculation of energy-transfer efficiencies of sample labeled fully with IAEDANS and acceptor. Assuming that labeling with the acceptor-bearing reagent is random at the three available sites of IAEDANS–enzyme, one can arrive at a set of equations which enables the computation of the transfer efficiency as a function of both the angles ϕ and θ and the incorporation level of acceptor. We find from such an analysis that essentially the same surface regions shown as allowed regions of Figure 6 occur as allowed regions for the range of experimentally evaluated efficiencies and incorporations appearing in Figure 5. The insensitivity of the catalytic-site loci to the degree of acceptor incorporation tends to substantiate the general structural conclusions reached earlier.

In summary, the energy-transfer experiments reported here suggest that the catalytic sites of UDPGDH are not in close proximity of each other. These sites are probably to be found, by techniques of higher resolution such as X-ray diffraction analysis of crystalline enzyme, on alternating poles of adjacent subunits or on other outer surface regions removed from the intersubunit bonding domains. Finally, these results relate to the recent communication of Eccleston et al. (1979) in which observations on the inactivation of UDPGDH caused by denaturant-induced dissociation are interpreted to mean that the catalytic-site thiol is close enough to a neighboring subunit to allow for intersubunit transfer of the aldehyde intermediate generated in the course of catalysis. Though there may be two subsites in each catalytic site, as proposed by these workers, the present energy-transfer results, cast in terms of the reasonable models developed herein, do not support the positioning of these two subsites on separate subunits. The allowed regions for the catalytic-site thiol (Figure 6) are too far from any neighboring subunit surface to account for a direct and rapid transfer of UDP-glucose aldehyde, bound as a Schiff's base on a lysine of a neighboring subunit, to the catalytic-site thiol.

References

Argauer, R. J., & White, C. E. (1964) *Anal. Chem. 36*, 368.

Azumi, T., & McGlynn, S. P. (1962) *J. Chem. Phys. 37*, 2413.

Bennett, J. C. (1967) *Methods Enzymol. 11*, 330.

Chen, R. F. (1967) *Anal. Biochem. 20*, 339.

Chen, R. F., & Bowman, R. L. (1965) *Science (Washington, D.C.) 147*, 729.

Cherry, R. J., & Schneider, G. (1976) *Biochemistry 15*, 3657.

Crestfield, A. M., Moore, S., & Stein, W. H. (1963) *J. Biol. Chem. 283*, 622.

Dale, R. E., Eisinger, J., & Blumberg, W. E. (1979) *Biophys. J. 26*, 161.

Dreyer, W. J., & Bynum, E. (1967) *Methods Enzymol. 11*, 32.

Eccleston, E. D., Thayer, M. L., & Kirkwood, S. (1979) *J. Biol. Chem. 254*, 11399.

Fairclough, R. H., & Cantor, C. R. (1978) *Methods Enzymol. 3*, 840.

Franzen, J. S., Kuo, I., Eichler, A. J., & Feingold, D. S. (1973) *Biochem. Biophys. Res. Commun. 50*, 517.

Franzen, J. S., Ishman, R., & Feingold, D. S. (1976) *Biochemistry 15*, 5665.

Franzen, J. S., Marchetti, P., Ishman, R., Ashcom, J., & Feingold, D. S. (1978) *Biochem. J. 173*, 701.

Franzen, J. S., Ashcom, J., Marchetti, P., Cardamone, J. J., Jr., & Feingold, D. S. (1980a) *Biochim. Biophys. Acta 614*, 242.

Franzen, J. S., Carrubba, C., Ashcom, J., Franzen, J. S., & Feingold, D. S. (1980b) *Fed. Proc., Fed. Am. Soc. Exp. Biol. 39*, 2074.

Franzen, J. S., Marchetti, P., & Feingold, D. S. (1980c) *Biophys. J. 32*, 223.

Gainey, P. A., & Phelps, C. F. (1974) *Biochem. J. 141*, 667.
Gainey, P. A., Pestell, T. C., & Phelps, C. F. (1972) *Biochem. J. 129*, 821.
Haas, E., Katchalski-Katzir, E., & Steinberg, I. Z. (1978a) *Biochemistry 17*, 5064.
Haas, E., Katchalski-Katzir, E., & Steinberg, I. Z. (1978b) *Biopolymers 17*, 11.
Huang, K., Fairclough, R. H., & Cantor, C. R. (1975) *J. Mol. Biol. 97*, 443.
Hudson, E. N., & Weber, G. (1973) *Biochemistry 12*, 4154.
Klotz, I. M., Darnall, D. W., & Langerman, N. R. (1975) *Proteins, 3rd Ed. 1*, 338–351.
Matthews, B. W., & Bernhard, S. A. (1973) *Annu. Rev. Biophys. Bioeng. 2*, 257.
Mercola, D. A., Morris, J. W. S., & Arquilla, E. R. (1972) *Biochemistry 11*, 3860.
Parker, C. A. (1968) in *Photoluminescence of Solutions*, pp 266, 267, Elsevier, New York.
Parker, C. A., & Rees, W. T. (1960) *Analyst (London) 85*, 587.
Rao, A., Martin, P., Rithmeier, A. F., & Cantley, L. C. (1979) *Biochemistry 18*, 4505.
Ridley, W. P., & Kirkwood, S. (1973) *Biochem. Biophys. Res. Commun. 54*, 955.
Ridley, W. P., Houchins, J. P., & Kirkwood, S. (1975) *J. Biol. Chem. 250*, 8761.
Scott, T. G., Spencer, R. D., Leonard, N. J., & Weber, G. (1970) *J. Am. Chem. Soc. 92*, 687.
Shinitzky, M. (1972) *J. Chem. Phys. 56*, 5979.
Stryer, L. (1978) *Annu. Rev. Biochem. 47*, 819.
Uram, M. (1971) *Fed. Proc., Fed. Am. Soc. Exp. Biol. 30*, 1319.
Uram, M., Bowser, A. M., Feingold, D. S., & Lamy, F. (1972) *An. Asoc. Quim. Argent. 60*, 135.
Vanderkooi, J. M., Ierokomas, A., Nakamura, H., & Martonosi, A. (1977) *Biochemistry 16*, 1262.
Wong, Y-H. H., Winer, F. B., & Frey, P. A. (1979) *Biochemistry 18*, 5332.
Zalitis, J., & Feinfold, D. S. (1968) *Arch. Biochem. Biophys. 132*, 457.

Substrate Specificity of the Collagenolytic Serine Protease from *Uca pugilator*: Studies with Noncollagenous Substrates†

Gregory A. Grant* and Arthur Z. Eisen

ABSTRACT: The collagenolytic serine protease (crab protease) isolated from the hepatopancreas of the fiddler crab, *Uca pugilator*, has been investigated with respect to its peptide bond specificity and catalytic properties by using noncollagenous substrates. In contrast to vertebrate collagenases, crab protease is a good general protease capable of degrading a variety of polypeptide and synthetic low molecular weight substrates. Crab protease displays a broad range of specificity, cleaving on the carboxyl-terminal side of residues with both positively and negatively charged side chains as well as hydrophobic side chains. The enzyme appears to favor tyrosyl, phenylalanyl, leucyl, and perhaps lysyl residues and, to a lesser extent, arginyl and glutamyl residues. The rate of cleavage of polypeptide substrates is similar to chymotrypsin but is significantly less than trypsin or chymotrypsin for low molecular weight esterase and amidase substrates. Crab protease is effectively inhibited by chymostatin but not by leupeptin or elastatinal. Several common chloromethyl ketone derivatives of phenylalanine and lysine are also ineffective, although crab protease efficiently cleaves at these residues in polypeptide substrates.

The collagenolytic protease isolated from the hepatopancreas of the fiddler crab, *Uca pugilator* (Eisen & Jeffrey, 1969; Eisen et al., 1970, 1973), has been shown by sequence analysis to be a serine protease (Grant et al., 1980) homologous to the pancreatic serine proteases of vertebrates. The first indication that this may be the case came from the observations that this enzyme possessed intrinsic trypsin- and chymotrypsin-like activity toward synthetic substrates and was inhibited by diisopropyl fluorophosphate and soybean trypsin inhibitor (Eisen et al., 1973). In addition to these activities, the enzyme had been shown to possess collagenolytic activity in that it cleaved native collagen under physiological conditions of pH, temperature, and ionic strength (Eisen & Jeffrey, 1969; Eisen et al., 1973). This was characterized by the cleavage of the native collagen helix at several sites in the area of the TC_{75}^{A} locus without loss of helical content. In addition, a marked decrease in the original intramolecular cross-linked β component of collagen with a corresponding increase in the monomeric α chains was also observed indicating an additional site of cleavage at the nonhelical ends of the molecule.

Since the fiddler crab is a scavenger that feeds on animal tissues frequently containing collagen, the presence of a collagenase in the hepatopancreas of these animals was not unexpected. However, most collagenases so far examined have been found to be metal-requiring neutral proteases (Seltzer et al., 1977). The crab protease was the first example of a serine protease that possessed significant collagenolytic activity. More recently, collagenolytic enzymes present in dog pancreas (Takahashi & Seifter, 1974), the fungus *Entomophthora coronata* (Hurion et al., 1979), and the insect *Hypoderma lineatum* (Lecroisey et al., 1979) have been reported which may also be serine proteases.

† From the Division of Dermatology, Department of Medicine, and the Department of Biological Chemistry, Washington University School of Medicine, St. Louis, Missouri 63110. *Received June 17, 1980.* This investigation was supported by U.S. Public Health Service Grants AM 12129 and AM 07284.

0006-2960/80/0419-6089$01.00/0